New Pressure Correction Equation for Incompressible Internal Flows

A. K. Mazher* and Don P. Giddens†
Georgia Institute of Technology, Atlanta, Georgia 30332

A space-marching method is employed to integrate the reduced form of the Navier-Stokes equations for steady incompressible viscous fluids for arbitrary three-dimensional internal flow geometries. The objective of this paper is to present the development of a new pressure correction equation that is used to correct the pressure and then the velocities locally at each marching station. The equation incorporates information from the momentum equations in the form of newly derived variables that are called V-P (velocity-pressure) variables. Although the momentum equations are solved as an uncoupled system, the V-P variables couple the equations indirectly through the solution of the new pressure correction equation. A numerical procedure based on this equation is used to sweep the entire domain in a stationwise manner. At each station one matrix inversion and a two-dimensional Poisson equation are required to satisfy the continuity and the momentum equations at the same time to conserve the volume flow rate. A computer code utilizing this procedure was tested for different geometries. Predictions of the flow through constricted and strongly curved pipes are in good agreement with previous experimental and computational results. As a result of using the V-P variables and the new pressure correction equation, CPU time is reduced.

Introduction

STEADY internal flows, where a dominant flow direction is identified, can be predicted by marching an approximate form of the Navier-Stokes equations along the main flow direction. The major difficulty in solving the steady Navier-Stokes equations for incompressible fluids as a parabolic system of equations is that these equations are actually elliptic in nature. The terms that prevent the equations from being parabolic in the main flow direction are the pressure gradient term and the viscous diffusion term. The pressure gradient term is very important and is always retained, while the viscous term is, in general, a small term and may often be neglected with little loss of accuracy. Various researchers[1-14] use different methods to treat the streamwise pressure gradient. While in Refs. 1 and 2 the continuity and momentum equations have been solved as a coupled system without employing the pressure correction equation, others[3-14] have employed a pressure correction equation.

In Ref. 3 a bulk streamwise pressure gradient is introduced and assumed to be uniform over the crossflow direction to ensure conservation of global volume flow rate. To ensure local conservation of mass flow, a pressure correction equation, which is derived from the continuity equation, is solved. A similar procedure has been used in Refs. 4 and 5, as far as the main flow pressure gradient is concerned, but this scheme requires the solution of two Poisson equations to ensure local mass conservation and to estimate the transverse pressure gradients. Other investigators[4-14] have developed similar methods to deal with the pressure gradient in the marching direction.

The major difficulty of these parabolic methods[3-14] is in satisfying mass conservation, local and global, through splitting the pressure term and solving a Poisson equation for the pressure. The momentum equations are solved as an uncoupled system, and thus an iterative procedure is required to accomplish the necessary coupling. The equation employed to couple the solution of the system of equations is a Poisson-type equation for the pressure or pressure corrections.

Since the interest of the present study was to solve for internal, incompressible steady flows through three-dimensional geometries, the idea of splitting the pressure into several contributions is used and generalized for curvilinear cases. This helps in satisfying the global volume flow rate that is important in internal flow calculations. Newly derived variables that relate the velocity correction to the pressure correction by a linear relation are defined. The uncoupled system is coupled locally at each station by using a new pressure correction equation of a Poisson type that employs the new variables. These variables, which are called V-P variables, are the coupling link between the momentum and the continuity equations. This results in the advantage that only one matrix inversion is required at each marching station. One feature of the preceding formulation is that the pressure correction equation and the relation between the velocity correction and the pressure correction are derived by using the full momentum equations without neglecting any term.

Mathematical Model

The equations describing three-dimensional, steady-state, incompressible, Newtonian, laminar flow in the nonconservative, nondimensional primitive variable formulation are the continuity equation,

$$\frac{\partial u}{\partial x} + \frac{\partial v}{\partial y} + \frac{\partial w}{\partial z} = 0 \tag{1}$$

and the momentum equations,

$$u\frac{\partial \phi}{\partial x} + v\frac{\partial \phi}{\partial y} + w\frac{\partial \phi}{\partial z} = -P_s + (1/R_e)\nabla^2\phi \tag{2}$$

where $P_s = \partial P/\partial s$. In the preceding formulation, the velocities are nondimensionalized by using the maximum inlet velocity W_{max}, and the Cartesian coordinates x, y, and z are nondimensionalized using the reference length D. The Reynolds number R_e is based on W_{max} and D. The symbol ϕ stands for any of the Cartesian velocities u, v, and w, and the subscript s represents the corresponding Cartesian coordinates x, y, and z. For the

Received Feb. 21, 1989; revision received March 16, 1990.

*Postdoctoral Fellow, School of Aerospace Engineering.
†Regents' Professor and Director, School of Aerospace Engineering.

pressure field P, the Poisson equation is employed

$$\nabla^2 P = -S_p \tag{3a}$$

where

$$S_p = \left(\frac{\partial u}{\partial x}\right)^2 + \left(\frac{\partial v}{\partial y}\right)^2 + \left(\frac{\partial w}{\partial z}\right)^2 + 2\left(\frac{\partial v}{\partial x}\frac{\partial u}{\partial y} + \frac{\partial v}{\partial z}\frac{\partial w}{\partial y} + \frac{\partial u}{\partial z}\frac{\partial w}{\partial x}\right)$$

with the normal pressure gradient P_n at the solid boundaries being computed from the normal momentum equation. In addition, the following integral constraint must be satisfied[4]

$$\iint_S P_n \, \mathrm{d}S = -\iiint_R S_p \, \mathrm{d}R \tag{3b}$$

where R is the integration region, and S is the surface bounding R.

To account for irregularities in geometry, an algebraic technique[15] is employed to generate transformed coordinates. Assume that any point (x,y,z) is transformed onto (ξ,η,ζ) according to the nonsingular transformations

$$x = x(\xi,\eta,\zeta)$$

$$y = y(\xi,\eta,\zeta)$$

$$z = z(\xi,\eta,\zeta)$$

By the chain rule of differentiation, the continuity equation becomes

$$\nabla \cdot V = \xi_x u_\xi + \eta_x u_\eta + \zeta_x u_\zeta + \xi_y v_\xi + \eta_y v_\eta + \zeta_y v_\zeta + \xi_z w_\xi + \eta_z w_\eta + \zeta_z w_\zeta = 0 \tag{4}$$

and the momentum equations become

$$U\phi_\xi + V\phi_\eta + W\phi_\zeta = -P_\phi + (1/R_e)(L_{\xi\xi} + L_{\eta\eta} + L_{\zeta\zeta})\phi + (1/R_e)(L_{\xi\eta} + L_{\xi\zeta} + L_{\eta\zeta})\phi \tag{5}$$

where

$$U = \xi_x u + \xi_y v + \xi_z w$$

$$V = \eta_x u + \eta_y v + \eta_z w$$

$$W = \zeta_x u + \zeta_y v + \zeta_z w$$

$$P_\phi = \xi_s P_\xi + \eta_s P_\eta + \zeta_s P_\zeta$$

and

$$L_{\xi\xi}(\phi) = \xi_x \partial_\xi(\xi_x \phi_\xi) + \xi_y \partial_\xi(\xi_y \phi_\xi) + \xi_z \partial_\xi(\xi_z \phi_\xi)$$

$$L_{\eta\eta}(\phi) = \eta_x \partial_\eta(\eta_x \phi_\eta) + \eta_y \partial_\eta(\eta_y \phi_\eta) + \eta_z \partial_\eta(\eta_z \phi_\eta)$$

$$L_{\zeta\zeta}(\phi) = \zeta_x \partial_\zeta(\zeta_x \phi_\zeta) + \zeta_y \partial_\zeta(\zeta_y \phi_\zeta) + \zeta_z \partial_\zeta(\zeta_z \phi_\zeta)$$

$$L_{\xi\eta}(\phi) = \xi_x \partial_\xi(\eta_x \phi_\eta) + \xi_y \partial_\xi(\eta_y \phi_\eta) + \xi_z \partial_\xi(\eta_z \phi_\eta) + \eta_x \partial_\eta(\xi_x \phi_\xi) + \eta_y \partial_\eta(\xi_y \phi_\xi) + \eta_z \partial_\eta(\xi_z \phi_\xi)$$

$$L_{\xi\zeta}(\phi) = \xi_x \partial_\xi(\zeta_x \phi_\zeta) + \xi_y \partial_\xi(\zeta_y \phi_\zeta) + \xi_z \partial_\xi(\zeta_z \phi_\zeta) + \zeta_x \partial_\zeta(\xi_x \phi_\xi) + \zeta_y \partial_\zeta(\xi_y \phi_\xi) + \zeta_z \partial_\zeta(\xi_z \phi_\xi)$$

$$L_{\eta\zeta}(\phi) = \eta_x \partial_\eta(\zeta_x \phi_\zeta) + \eta_y \partial_\eta(\zeta_y \phi_\zeta) + \eta_z \partial_\eta(\zeta_z \phi_\zeta) + \zeta_x \partial_\zeta(\eta_x \phi_\eta) + \zeta_y \partial_\zeta(\eta_y \phi_\eta) + \zeta_z \partial_\zeta(\eta_z \phi_\eta)$$

and U, V, and W are the contravariant velocities. The operators $L_{\xi\eta}$, $L_{\xi\zeta}$, and $L_{\eta\zeta}$ become zeros in an orthogonal coordinate system of axes. The pressure equation transforms to

$$L_{\xi\xi}(P) + L_{\eta\eta}(P) + L_{\zeta\zeta}(P) + L_{\xi\eta}(P) + L_{\xi\zeta}(P) + L_{\eta\zeta}(P) = -\bar{S}_p(\xi,\eta,\zeta)$$

where $\bar{S}_p(\xi,\eta,\zeta)$ is computed from S_p, Eq. (3a), by using the chain rule. The normal pressure gradient at the solid boundaries P_n is computed from the transformed momentum equations.

Present Method

The present method uses the reduced Navier-Stokes equations to march the solution along the main flow direction. The pressure term is split into three parts, and these parts are computed to satisfy local and global mass conservation. Multiple sweeps or passes are considered for large elliptic effects, and for such cases the velocities are stored only in the separated region while the entire pressure field is stored. A set of newly derived variables is defined and calculated as a byproduct of solving the uncoupled momentum equations. These variables represent a coupling link between the momentum and continuity equations and are employed to derive a new pressure correction equation that is solved at each marching station to satisfy the local mass continuity.

For internal flows let the ζ coordinate be in the main flow direction and neglect the diffusion terms in this direction. The pressure term is split into three parts

$$P(\xi,\eta,\zeta) = PP(\xi,\eta,\zeta) + \bar{P}(\zeta) + p(\xi,\eta;\zeta) \tag{6}$$

where

$$PP(\xi,\eta,\zeta) = \begin{cases} P_0(\xi,\eta,\zeta) & \text{in the first pass} \\ P^n(\xi,\eta,\zeta) & \text{in the other passes} \end{cases}$$

such that

$$\lim_{n \to N} \|\bar{P}\| \le \epsilon$$

$$\lim_{n \to N} \|p(\xi,\eta,\zeta)\| \le \delta$$

$$\lim_{n \to N} P^n(\xi,\eta,\zeta) \to P(\xi,\eta,\zeta)$$

where ϵ and δ are small real numbers.

One part, $\bar{P}$, which is a function of ζ only, is calculated so that the total volume flow rate is conserved at each station. The second part, $PP = P_0$, is the one-dimensional pressure solution that is a function of area changes in the main flow direction as computed from Bernoulli's equation or the potential pressure solution for the same geometry, if it is known. The potential pressure is used in the first pass only, while $PP = P^n$, which is solution of the three-dimensional Poisson equation from the previous pass, is used in the other passes after the first. In this case, the pressure PP gives some information regarding the elliptic nature of the problem. The third part, p, is the transverse pressure correction at a given ζ location, which is a function of ξ and η.

With the preceding assumption, the momentum equations, (5) become

$$W\phi_\zeta = -P_\phi + (1/R_e)L_{\xi\xi}(\phi) - U\phi_\xi + (1/R_e)L_{\eta\eta}(\phi) - V\phi_\eta + (1/R_e)\left[L_{\xi\eta}(\phi) + L_{\xi\zeta}(\phi) + L_{\eta\zeta}(\phi)\right] \tag{7}$$

where

$$P_\phi = \xi_s\left(\frac{\partial PP}{\partial \xi} + \frac{\partial p}{\partial \xi}\right) + \eta_s\left(\frac{\partial PP}{\partial \eta} + \frac{\partial p}{\partial \eta}\right) + \zeta_s\left(\frac{\partial PP}{\partial \zeta} + \frac{\mathrm{d}\bar{P}}{\mathrm{d}\zeta}\right)$$

Difference Equations

A finite-difference scheme is used to discretize the momentum equations. The nonlinear convective terms are linearized by using the upstream stations. In the reversed flow regions, the FLAIR approximation is employed in the first pass while upwinding schemes are used in the other passes. Central differences are employed for the viscous terms. A forward-difference scheme is used for the pressure gradient term in the main flow direction after the first pass. With these difference formulas, the momentum equation becomes

$$\Delta_\phi \phi_{i,j,k+1} = R_\phi - \xi_s \frac{\partial p}{\partial \xi} - \eta_s \frac{\partial p}{\partial \eta} - \zeta_s \frac{\mathrm{d}\bar{P}}{\mathrm{d}\zeta} \tag{8}$$

where Δ_ϕ is a finite-difference operator and is the same for all momentum equations. At each station, Eq. (8) can be written in a matrix form as follows

$$[A]\{\phi\} = \{RHS\}$$

To advance the solution from station k to station $k+1$ by the space-marching method, only one matrix inversion is required for the three momentum equations. This will result in the correct solution if the $\{RHS\}$ is given accurately, but the $\{RHS\}$ is dependent on $\bar{P}_\zeta$ and p_ξ and p_η, which are not known in advance. A procedure to calculate these pressures will be discussed shortly.

Calculation Procedure for $\mathrm{d}\bar{P}/\mathrm{d}\zeta$

The numerical value of $\mathrm{d}\bar{P}/\mathrm{d}\zeta$ at each station is computed to satisfy the inlet volume flow rate Q_{in}, by assuming values of p_ξ, p_η, and $\mathrm{d}\bar{P}/\mathrm{d}\zeta$ (let these values be p_ξ^*, p_η^*, and $\mathrm{d}\bar{P}^*/\mathrm{d}\zeta$) and marching equation, Eq. (8), from station k to station $k+1$ to obtain u_1, v_1, and w_1. The velocities u_1, v_1, and w_1 and the $\mathrm{d}\bar{P}^*/\mathrm{d}\zeta$ term are corrected to satisfy the inlet volume flow rate by assuming

$$\phi^* = \phi_1 + \mathrm{d}\phi_1$$

$$\mathrm{d}\phi_1 = \frac{\partial \phi_1}{\partial P_\zeta} \cdot DP_\zeta$$

$$\mathrm{d}\bar{P}/\mathrm{d}\zeta = \mathrm{d}\bar{P}^*/\mathrm{d}\zeta + DP_\zeta \tag{9}$$

the volume flow rate is computed from W using Eq. (9),

$$W = W(\mathrm{d}\bar{P}/\mathrm{d}\zeta) = W_1 + DW_1$$

$$DW_1 = \frac{\partial W}{\partial P_\zeta} \cdot DP_\zeta = \left(\zeta_x \frac{\partial u}{\partial P_\zeta} + \zeta_y \frac{\partial v}{\partial P_\zeta} + \zeta_z \frac{\partial w}{\partial P_\zeta}\right) \cdot DP_\zeta \tag{10}$$

where W_1 is the value of W calculated with the guessed pressure gradients. To calculate $\partial W/\partial P_\zeta$, Eq. (8) is differentiated with respect to $\mathrm{d}\bar{P}/\mathrm{d}\zeta$ to obtain the following partial differential equations

$$\Delta_\phi u_{p_\zeta} = -\zeta_x$$

$$\Delta_\phi v_{p_\zeta} = -\zeta_y$$

$$\Delta_\phi w_{p_\zeta} = -\zeta_z \tag{11}$$

with zero values at the solid boundaries and $\phi_{p_\zeta} = \partial\phi/\partial P_\zeta$.

Comparison of Eqs. (8) and (11) shows that one matrix inversion is required to solve both equations. To calculate DP_ζ, Eq. (10) is integrated over the cross section at the station $k+1$ to obtain, since DP_ζ is constant at a given station,

$$DP_{\zeta_{k+1}} = \frac{Q_{\text{in}} - Q_{1(k+1)}}{\displaystyle\iint_{A_{k+1}} \frac{\partial W}{\partial P_\zeta}\,\mathrm{d}\xi\,\mathrm{d}\eta} \tag{12}$$

The correct main flow velocity W_{k+1} and the pressure gradient $\mathrm{d}\bar{P}/\mathrm{d}\zeta$ are then calculated from Eqs. (8–12).

Calculation Procedure for $p(\xi,\eta,\zeta)$

The solution of Eq. (8) with guessed values of p_ξ, p_η, and the correct value of $\mathrm{d}\bar{P}/\mathrm{d}\zeta$ is denoted by $\phi^* = u^*$ or v^* or w^*. These velocities are calculated to conserve the inlet volume flow rate Q_{in} as just described. In this case, Eq. (8) becomes

$$\Delta_\phi u^* = R_u - \xi_x \frac{\partial p^*}{\partial \xi} - \eta_x \frac{\partial p^*}{\partial \eta} - \zeta_x \frac{\mathrm{d}\bar{P}}{\mathrm{d}\zeta}$$

$$\Delta_\phi v^* = R_v - \xi_y \frac{\partial p^*}{\partial \xi} - \eta_y \frac{\partial p^*}{\partial \eta} - \zeta_y \frac{\mathrm{d}\bar{P}}{\mathrm{d}\zeta}$$

$$\Delta_\phi w^* = R_w - \xi_z \frac{\partial p^*}{\partial \xi} - \eta_z \frac{\partial p^*}{\partial \eta} - \zeta_z \frac{\mathrm{d}\bar{P}}{\mathrm{d}\zeta} \tag{13}$$

The values of u^*, v^*, and w^* will not satisfy the continuity equation (4) unless p^* is the correct pressure. Therefore, corrections to the velocities u^*, v^*, and w^* and the pressure p^* are assumed to satisfy the continuity and the momentum equations, i.e.,

$$\phi = \phi^* + \phi_c$$

$$p = p^* + p_c \tag{14}$$

Substituting these values into Eq. (8) and subtracting Eq. (13) from the resulting equation gives

$$\Delta_\phi \phi_c = -\xi_s \frac{\partial p_c}{\partial \xi} - \eta_s \frac{\partial p_c}{\partial \eta} \tag{15}$$

Equation (15) is locally linear and inhomogeneous with the pressure gradients p_{c_ξ} and p_{c_η} as forcing functions. The solution of this equation can be assumed as

$$\phi_c = \phi_{p_\xi} \cdot p_{c_\xi} + \phi_{p_\eta} \cdot p_{c_\eta}$$

From this, six variables can be defined that represent the velocity field at each station due to unit transverse pressure gradients. These variables are defined as follows,

$$u_{p_\xi} = \frac{\partial u}{\partial p_\xi}, \qquad u_{p_\eta} = \frac{\partial u}{\partial p_\eta}$$

$$v_{p_\xi} = \frac{\partial v}{\partial p_\xi}, \qquad v_{p_\eta} = \frac{\partial v}{\partial p_\eta}$$

$$w_{p_\xi} = \frac{\partial w}{\partial p_\xi}, \qquad w_{p_\eta} = \frac{\partial w}{\partial p_\eta} \tag{16}$$

To compute these, Eq. (8) is differentiated with respect to p_ξ and p_η, respectively. The resulting equations are

$$\Delta_\phi u_{p_\xi} = -\xi_x, \qquad \Delta_\phi u_{p_\eta} = -\eta_x$$

$$\Delta_\phi v_{p_\xi} = -\xi_y, \qquad \Delta_\phi v_{p_\eta} = -\eta_y$$

$$\Delta_\phi w_{p_\xi} = -\xi_z, \qquad \Delta_\phi w_{p_\eta} = -\eta_z \tag{17}$$

The left-hand side of Eq. (17) is the same as that of Eqs. (8) and (11). Then one matrix inversion is required to solve Eqs.

(8), (11), and (17). Solution of Eqs. (17) gives the velocity corrections as

$$\phi_c = \begin{cases} u_c = u_{p_\xi} p_{c_\xi} + u_{p_\eta} p_{c_\eta} \\ v_c = v_{p_\xi} p_{c_\xi} + v_{p_\eta} p_{c_\eta} \\ w_c = w_{p_\xi} p_{c_\xi} + w_{p_\eta} p_{c_\eta} \end{cases} \tag{18}$$

Notice the role of the V-P variables, Eq. (16), as information sources from the momentum equations. Substituting Eq. (14) into the continuity equation, Eq. (4), using Eq. (18), and arranging the terms results in the following equation for the pressure correction:

$$L_{\xi\xi}(p_c) + L_{\xi\eta}(p_c) + L_{\eta\eta}(p_c) = -\nabla \cdot V^* \tag{19}$$

where

$$L_{\xi\xi}(p_c) = \xi_x \partial_\xi (u_{p_\xi} p_{c_\xi}) + \xi_y \partial_\xi (v_{p_\xi} p_{c_\xi}) + \xi_z \partial_\xi (w_{p_\xi} p_{c_\xi})$$

$$L_{\eta\eta}(p_c) = \eta_x \partial_\eta (u_{p_\eta} p_{c_\eta}) + \eta_y \partial_\eta (v_{p_\eta} p_{c_\eta}) + \eta_z \partial_\eta (w_{p_\eta} p_{c_\eta})$$

$$L_{\xi\eta}(p_c) = \xi_x \partial_\xi (u_{p_\eta} p_{c_\eta}) + \xi_y \partial_\xi (v_{p_\eta} p_{c_\eta}) + \xi_z \partial_\xi (w_{p_\eta} p_{c_\eta})$$

$$+ \eta_x \partial_\eta (u_{p_\xi} p_{c_\xi}) + \eta_y \partial_\eta (v_{p_\xi} p_{c_\xi}) + \eta_z \partial_\eta (w_{p_\xi} p_{c_\xi})$$

In deriving this equation, the main flow velocity correction is considered zero to conserve the volume flow rate, as outlined before, and V^* is the corresponding velocity as calculated from the momentum equations. This pressure correction equation is different from the pressure correction equations derived previously in the literature.[3-5,7-10] Also, this equation links the momentum equations with the continuity equation through the newly defined set of V-P variables of Eq. (16) and gives the pressure correction required to satsify the momentum and the continuity equations locally at each station k. The boundary condition for p_c is a zero normal derivative on the solid boundaries. The right-hand side of Eq. (19) is the mass source as computed from the continuity equation. If u^*, v^*, and w^* satisfy the continuity equation, then the solution of Eq. (19) with zero on the right-hand side and with zero boundary condition is zero or a constant value. Solving Eq. (19), u_c, v_c, and w_c can be calculated from Eq. (18).

Solution Procedure

Starting from the given inlet conditions, the following steps are performed for each station k.

1) Assume values for p_ξ, p_η, and $\mathrm{d}\bar{P}/\mathrm{d}\zeta$, then solve Eqs. (8), (11), and (17) for u_1, v_1, w_1, u_{p_ξ}, u_{p_η}, u_{p_ζ}, v_{p_ξ}, v_{p_η}, v_{p_ζ}, w_{p_ξ}, w_{p_η}, and w_{p_ζ} by using only one matrix inversion.

2) Compute DP_ζ from Eq. (12).

3) Compute u^*, v^*, and w^* from steps 1 and 2, and Eq. (9).

4) Solve Eq. (19) for p_c, which is a two-dimensional elliptic equation.

5) Correct the velocities using Eqs. (14) and (18).

6) Use these values to advance the solution to the next marching station.

7) When the downstream is reached, the entire pressure field is updated by solving the complete three-dimensional Poisson equation for the pressure.

8) The PP term in the momentum equation, as an approximate solution of the pressure computed from the previous step, is considered as a source term and is used for marching the solution from the inlet to the outlet. The PP_ζ term is forward differenced in this case, and the velocities in the reversed flow region are stored for the other passes. Steps 1-7 are repeated until the velocities resulting from the momentum equations satisfy the continuity equation within a certain error range.

Computational Results

A computer program has been written using the procedure just described. As a verification of the computational scheme, the code has been tested for three cases. The first case is the fully developed flow through a straight pipe, the second case is the flow through a constricted pipe, and the third case is the flow through a curved pipe. These one-, two-, and three-dimensional problems, respectively, were selected to check the ability of the code to recover the flowfield of simple flows by using the complete three-dimensional formulation in curvilinear coordinates. In each case, circular cross sections were employed, and the equations were solved for the complete geometry. The code successfully solved for the flowfield and recovered the symmetry. The results are in good agreement with the existing data. The results of case two and three are discussed in more detail below.

Case I: Flow Through a Constricted Pipe

For case I, a two-dimensional flow problem was solved by employing the three-dimensional code. In previous studies,[16-18] the vorticity-stream function formulations were used to solve for flow in a two-dimensional axisymmetric constricted pipe. In the present work, a complete three-dimensional formulation in primitive variables is employed to solve constricted pipe problems. Figure 1 shows the geometry. In this case, Z_0 is 4 and α is two-thirds with 89% area reduction. A sheared Cartesian grid ($11 \times 24 \times 110$) was used in the ξ, η, and ζ directions. The points were uniformly distributed in η and ζ, while they were exponentially distributed in the ξ direction. The program was run for three different Reynolds numbers that cover the unseparated to separated ranges. The results were compared with existing numerical results,[17,18] and comparison was good within the computational accuracy of the coarse mesh employed in the calculations. Because the area reduction is large (89%), the separation starts at a very low Reynolds number that is 17.5 in this geometry. Thus, the Reynolds numbers considered were 6, 17.5, and 25. Figures 2a–2d depict the results of the separated case for $R_e = 25$. In all of these figures, the computed results were compared with the vorticity stream function numerical data,[17,18] and the comparisons were acceptable. Figure 2a shows the axial velocity profile development at the plane of symmetry for $R_e = 25$. From the figure it is seen that the velocity profiles develop smoothly, and the separation region is clear at this small Reynolds number. Also, the two-dimensional axisymmetric flowfield of this problem was recovered. The centerline axial velocity is depicted in Fig. 2b where the comparison shows acceptably small differences in the region downstream of the constriction. Figure 2c shows the wall shear stress distribution in the ζ direction. Comparison with Ref. 17 is shown and is good for this Reynolds number. Figure 2d depicts the static pressure variation at the centerline of the stenosis. The comparison is good downstream of the constriction, but there are small differences upstream of the constriction. One pass is required to solve this problem where the error in the mass sources is of order 10^{-2}. The mass sources were calculated at every plane as the summation of the absolute value of the continuity equation evaluated at each point in the

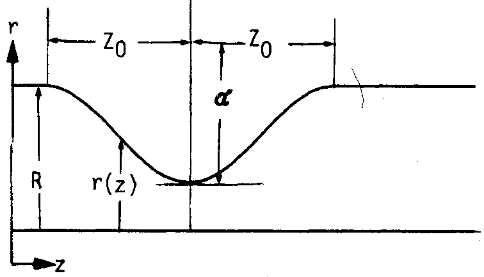

Fig. 1 Geometry of pipe with smooth constriction.

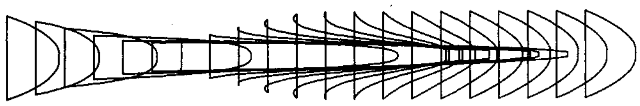

Fig. 2a Velocity profiles at the plane of symmetry, case I, $R_e = 25$.

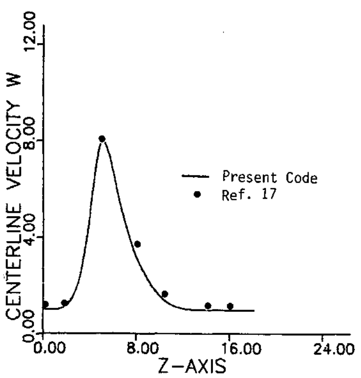

Fig. 2b Centerline velocity distribution along the axial direction, case I, $R_e = 25$.

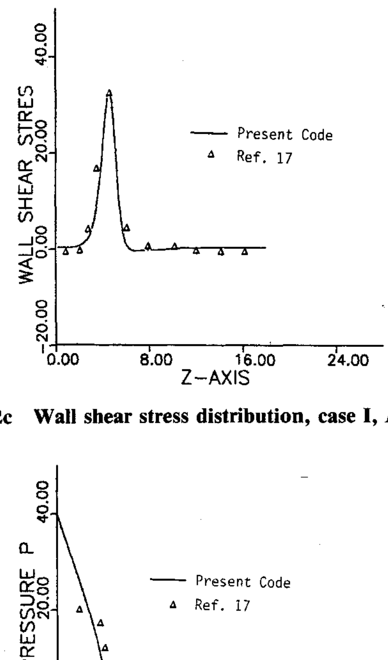

Fig. 2c Wall shear stress distribution, case I, $R_e = 25$.

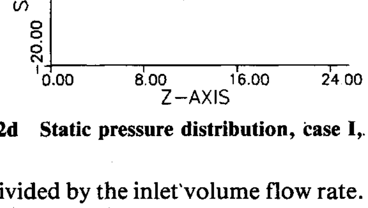

Fig. 2d Static pressure distribution, case I, $R_e = 25$.

plane and divided by the inlet volume flow rate. The CPU time per point in this problem was 0.04 s.

Case II: Flow Through a Curved Pipe

A three-dimensional problem represented by a curved pipe was solved to test the ability of the procedure to treat three-dimensional problems and to predict secondary flow patterns. Figure 3 presents the geometry and shows the notations used in presenting the results. In this geometry, the curvature ratio is given by $\lambda = a/R_c = 1/7$, the Dean number is $K = 2R_e\sqrt{\lambda} = 183$ with uniform inlet profile. Data from an experimental study[19] were used for comparison with the results of the present code. In the following figures, the velocities were nondimensional-

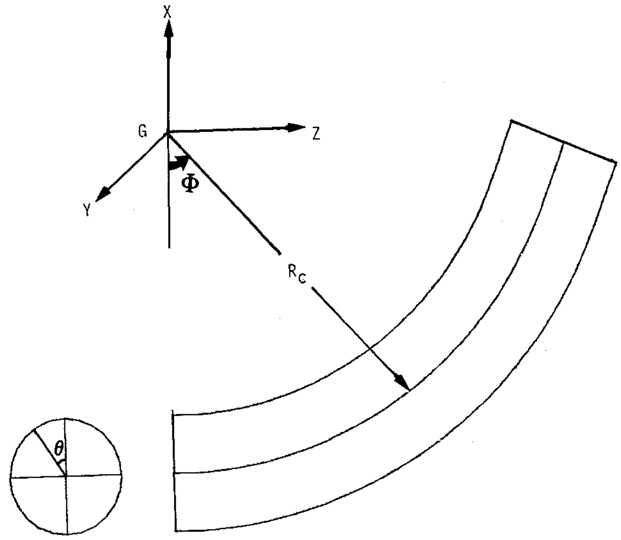

Fig. 3 Geometry and coordinates for a curved pipe.

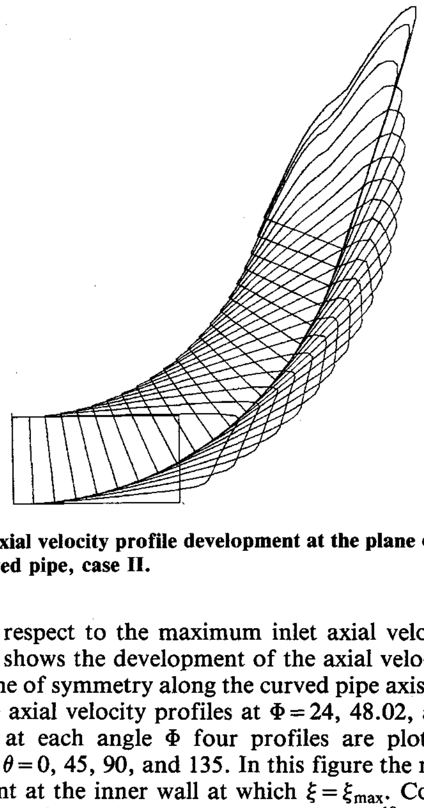

Fig. 4a Axial velocity profile development at the plane of symmetry of the curved pipe, case II.

ized with respect to the maximum inlet axial velocity W_{max}. Figure 4a shows the development of the axial velocity profile at the plane of symmetry along the curved pipe axis. Figure 4b shows the axial velocity profiles at $\Phi = 24$, 48.02, and 61.115 deg, and at each angle Φ four profiles are plotted at the diagonals $\theta = 0$, 45, 90, and 135. In this figure the radius $r = 0$ is the point at the inner wall at which $\xi = \xi_{max}$. Comparisons with the experimental results of Agarwal et al.[19] are shown in Fig. 5 at three angles $\Phi = 15.1$, 30, and 60 where the profiles are compared at the angle $\theta = 0$. The comparison is satisfactory for the coarse mesh employed. The distribution and the number of the grid points are the same as in the previous case. In this problem 110 stations were used, which covered the flowfield from $\Phi = 0$ to 65.8. The CPU time per point was 0.0452 s.

Discussion and Conclusions

The work presented in this paper uses a space-marching technique to integrate the three-dimensional Navier-Stokes equations for laminar, steady, incompressible internal flows through general three-dimensional geometries. The momentum equations are marched from the given inlet to the outlet, by neglecting the diffusion terms in the main flow direction. Although this idea has been used before,[7,8] the equation used to treat the velocity-pressure coupling by satisfying the conti-

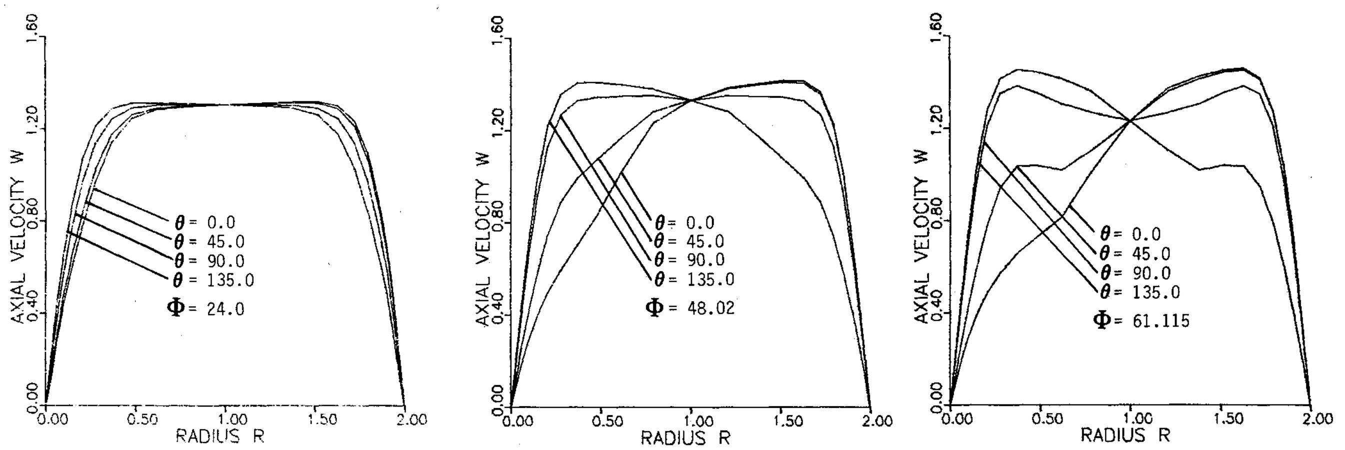

Fig. 4b Axial velocity profiles, case II, at $\Phi = 24$, 48.02, and 61.115 deg.

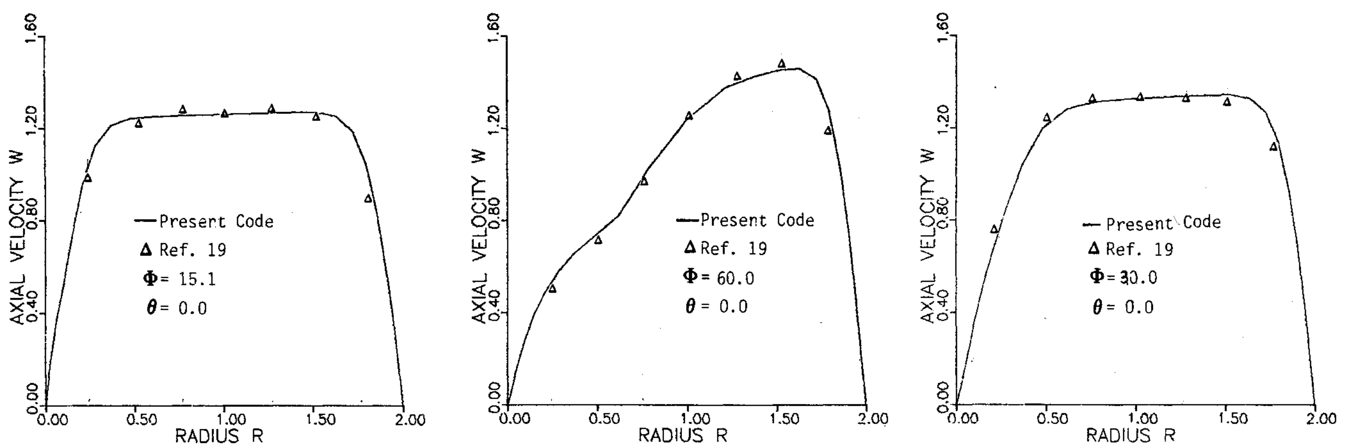

Fig. 5 Axial velocity profile comparison, case II, at $\Phi = 15.1$, 30, and 60 deg.

nuity equation represents a new equation to couple the Navier-Stokes equations for incompressible internal flows.

The unknown pressure distribution in the primitive variable formulation represents a difficult problem for incompressible flows. The continuity equation must be handled so as to ensure a converged solution of the coupled system of continuity and momentum equations and to conserve the total volume flow at each station. To treat this problem by conserving the volume flow rate while at the same time satisfying the continuity equation and keeping the elliptic effects, the pressure is split into three parts. One part, which is responsible for the volume flow rate, i.e., the pressure in the main flow direction, is calculated in such a way that the volume flow rate is conserved at each streamwise station. In this way, part of the elliptic effect in main flow direction is taken into consideration. The second part of the pressure is taken from the one-dimensional Bernoulli's equation. This represents the elliptic effects due to the area changes. Despite this approximation, this term represents first-order effects of the changing geometry in the main flow direction. The third part of the pressure is considered as a correction part at every cross section and computed to satisfy the continuity equation locally. The transverse velocities in the cross-sectional planes are influenced by this part.

This splitting decouples the solution for pressure from the momentum equations, and the velocities can be calculated at each station by a marching procedure. The equation developed to calculate the transverse pressure and hence to compute the transverse velocity is new. In developing this equation, six derived variables are introduced and called the velocity-pressure variables. Their calculation is a byproduct of the marching scheme so that no additional effort is needed. The V-P variables are solutions of the linearized Navier-Stokes equation that are independent of the unknown pressure field of the given problem. They represent a source of information about the flowfield for given geometry. Further research is needed to learn their usefulness, and the relation of these variables to the Green function of the corresponding partial differential equation should be explored.

The entire procedure was checked by solving one-, two-, and three-dimensional problems. The comparisons are good with the analytical, computed, and experimental results available in the literature.

References

[1]Rubin, S. G., and Reddy, D. R., "Analysis of Global Pressure Relaxation for Flows with Strong Interaction and Separation," *Computers and Fluids,* Vol. 11, No. 4, 1983, pp. 281–306.

[2]Rubin, S. G., and Reddy, D. R., "Global PNS Solution for Laminar and Turbulent Flow," AIAA Paper 83-1911, July 1983.

[3]Patankar, S. V., and Spalding, D. B., "A Calculation Procedure for Heat, Mass and Momentum Transfer in Three-Dimensional Flows," *International Journal of Heat and Mass Transfer,* Vol. 15, Pt. 2, Oct. 1972, pp. 1787–1806.

[4]Briley, W. R., "Numerical Method For Predicting Three-Dimensional Steady Viscous Flow In Ducts," *Journal of Computational Physics,* Vol. 14, No. 1, Jan. 1974, pp. 8–28.

[5]Ghia, U., Ghia, K. N., and Studerus, C. J., "Three-Dimensional Laminar Incompressible Flow in Straight Polar Ducts," *Computers and Fluids,* Vol. 5, No. 4, 1977, pp. 205–218.

[6]Madavan, N. K., and Pletcher, R. H., "Prediction of the Incompressible Separated Flows Using a Partially Parabolized Navier-Stokes Equations," Iowa State University, College of Engineering, Ames, IA, TR HTL-27 CFD-5, Feb. 1982.

[7]Khalil, I. M., and Weber, H. G., "Modeling of Three-Dimensional Flow in Turning Channels," *Journal of Engineering for Gas Turbines*

and Power, Vol. 106, No. 3, July 1984, pp. 682–691.

[8]Rhie, C. M., "Basic Calibration of a Partially-Parabolic Procedure Aimed at Centrifugal Impeller Analysis," AIAA Paper 83-0260, Jan. 1983.

[9]Roberts, D. W., and Forester, C. K., "Parabolic Procedure For Flows In Ducts With Arbitrary Cross Section," *AIAA Journal,* Vol. 17, No. 1, 1979, pp. 33–40.

[10]Raithby, G. D., and Schneider, G. E., "Numerical Solution of Problems In Incompressible Fluid Flow: Treatment of the Velocity-Pressure Coupling," *Numerical Heat Transfer,* Vol. 2, No. 4, 1979, pp. 417–440.

[11]Ghia, K. H., and Sokhey, J. S., "Analysis and Numerical Solution of Viscous Flow in Curved Ducts of Regular Cross-Sections," *Numerical/Laboratory Computer Methods in Fluid Mechanics,* edited by A. A. Pouring and V. L. Shah, ASME, New York, 1976, pp. 53–71.

[12]Kirtley, K. R., and Lakshminarayana, B., "Computation of Internal Incompressible Separated Flows Using a Space-Marching Technique," AIAA Paper 84-1624, July 1985.

[13]Pouagare, M., and Lakshminarayana, B., "A Space-Marching Method for Viscous Incompressible Internal Flows," *Journal of Computational Physics,* Vol. 64, No. 2, June 1986, pp. 389–415.

[14]Ghia, U., Ghia, K. N., Rubins, S. G., and Khosla, P. K., "Study of Incompressible Flow Separation Using Primitive Variables," *Computers and Fluids,* Vol. 9, No. 2, 1981, pp. 123–142.

[15]Mazher, A. K., and Giddens, D. P., "A Fast Algebraic Technique to Generate 2D and 3D Grids for Computation of Hemodynamic Studies," *Proceedings of ASME Bioengineering Spring Conference,* ASME, New York, Vol. 84, June 1987, pp. 61–64.

[16]Lee, S. J., and Fung, C. Y., "Flow in Locally Constricted Tubes at Low Reynolds Numbers," *Journal of Applied Mechanics,* Vol. 37, No. 1, March 1970, pp. 9–16.

[17]Deshpande, M. D., "Steady and Turbulent Flow Through Vascular Stenosis Models," Ph.D. Thesis, Georgia Institute of Technology, Atlanta, GA, June 1977.

[18]Deshpande, M. D., Giddens, D. P., and Mabon, R. F., "Steady Laminar Flow Through Modeled Vascular Stenoses," *Journal of Biomechanics,* Vol. 9, No. 4, 1976, pp. 165–174.

[19]Agarwal, Y., Talbot, L., and Gong, K., "Laser Anemometer Study of Flow Development in Curved Circular Pipes," *Journal of Fluid Mechanics,* Vol. 85, Pt. 3, April 1978, pp. 497–518.